Vol 18 No 7, July 2009
1674-1056/2009/18(07)/3049-05

Chinese Physics B

© 2009 Chin. Phys. Soc.
and IOP Publishing Ltd

Cavity design and linear analysis of 225 GHz frequency-quadrupling gyroklystron*

Liu Di-Wei(刘頓威)†, Yuan Xue-Song(袁学松),
Yan Yang(鄢 扬), and Liu Sheng-Gang(刘盛纲)

THz Research Center, Research Institute of High Energy Electronics, University of Electronic Science and Technology of China, Chengdu 610054, China

(Received 18 November 2008; revised manuscript received 23 December 2008)

This paper considers the frequency-quadrupling three-cavity gyroklystrons with successive frequency-doubling in each cavity. The cavities of 225 GHz frequency-quadrupling gyroklystron are designed with the scattering matrices method and the possible operating mode are discussed. With the point-gap theory, the starting currents of the possible operating modes and the potential parasitic modes in the output cavity are calculated. The optimal operating mode is proposed under consideration of the mode competition and the power capacity of the cavity.

Keywords: frequency-quadrupling gyroklystron, THz, scattering matrices, point-gap theory
PACC: 7640, 4110H, 5270G

1. Introduction

There is a strong interest in developing compact high power sources of coherent electromagnetic radiation in the submillimeter wave and THz regions.[1] Gyrotrons are known as the most powerful sources of radiation in this frequency range.[2−4] However the gyrotron operating at fundamental cyclotron resonance at these frequencies requires large cryomagnets or superconducting magnets producing strong enough magnetic fields. To realize gyrotron operation at higher frequency and to use more compact and less expensive magnets and cryomagnets, it seems expedient to consider the cyclotron harmonic gyrotron.[5,6] In this article, 225 GHz frequency-quadrupling three-cavity gyroklystron with successive frequency-doubling in each cavity is considered. The cavity's design with scattering matrices method and the mode competition with point-gap theory are discussed in details. The optimal operating mode in the output cavity is proposed under consideration of the mode competition and the power capacity of the cavity.

2. Elements of the theory

2.1. Cavity design with scattering matrices

The output cavity structure of the gyroklystron is shown in Fig.1, where ϕ, $R_{\rm W}$, L_1, L_2 is the angle, the radius and the length of the output cavity, respectively; $S_{\rm L}$, $S_{\rm R}$ are the left and right scattering matrices due to the abrupt change of the cavity radius, respectively. Using the scattering matrices formulation,[7]

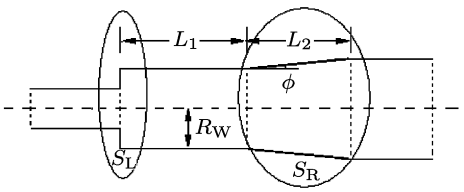


Fig.1. Structure of the output cavity.

we easily obtain the scattering matrices $S_{\rm L}$, $S_{\rm R}$. According to the resonant condition[8]

$$2\beta_{\rm mn}L + \theta_{\rm L} + \theta_{\rm R} = 2N\pi, \tag{1}$$

we can obtain the resonant frequency ω of the cavity. Where $\theta_{\rm L}$ and $\theta_{\rm R}$ are the phases of the operating mode's reflection coefficient $\Gamma_{\rm L}$, $\Gamma_{\rm R}$, which can be obtained from scattering matrices $S_{\rm L}$, $S_{\rm R}$, respectively, $\beta_{\rm mn}$ is the propagating constant. The diffractive quality factor $Q_{\rm d}$ can be written as[8]

$$Q_{\rm d} = v_{\rm g}\frac{2\omega L}{\left(1-|\Gamma_{\rm L}|^2\,|\Gamma_{\rm R}|^2\right)}. \tag{2}$$

*Project supported by National Natural Science Foundation of China (Grant No 10676110) and National High Technology Research and Development Program of China (Grant No 2007BC310401).
†E-mail: dwliu212220@163.com

Here $v_{\rm g}$ is the group velocity. Ohmic quality factor $Q_{\rm o}$ can be approximately expressed as[5]

$$Q_{\rm o} = \frac{R}{\delta}\left(1 - \frac{m^2}{u_{\rm mn}^2}\right). \tag{3}$$

Here $\delta \approx \sqrt{2/\omega\mu\sigma}$ is the skin-depth. For practical purposes the conductivity σ is often taken as half the theoretical value that corresponds to the account of the surface roughness of the wall. The total quality factor $Q_{\rm T}$ can be written as

$$Q_{\rm T} = \frac{Q_{\rm o}Q_{\rm d}}{Q_{\rm o} + Q_{\rm d}}. \tag{4}$$

The mode profile can also be easily obtained by using the scattering matrices formulation.[7] Using the same methods discussed here, we can also obtain the resonant frequencies and the mode profiles of the input cavity and the bunching cavity.

2.2. Point-gap theory

To simplify our task, we will consider weakly relativistic electron beams and neglect space charge effects. For the case when electrons interact with electromagnetic fields excited at frequencies near the cutoff frequency, the electron motion can be described by the following sets of equations:[9,10]

$$\begin{aligned} &\frac{{\rm d}\varepsilon}{{\rm d}t} = -e\boldsymbol{v}\cdot\boldsymbol{E}, \\ &\frac{{\rm d}\boldsymbol{p}}{{\rm d}t} + \eta\boldsymbol{v}\times\boldsymbol{B}_0 = -\eta\boldsymbol{E} = \boldsymbol{a}. \end{aligned} \tag{5}$$

Here ε is the electron energy, $\boldsymbol{p} = \gamma\boldsymbol{v}_\perp$ is the electron momentum, γ is the relativistic factor, $\eta = e/m_0$ is the ratio between electron charge and mass. In the approximation of the fixed Gaussian longitudinal structure of the high-frequency field in the cavity

$$f(z) = \exp\left[-(2z/L)^2\right]. \tag{6}$$

From Eq.(5) we can obtain the starting current expression of $\rm TE_{mn}$ mode for the zero velocity spread,[11]

$$\frac{0.465Q_{\rm T}I_{\rm st}LG_{\rm mn}\beta_{\perp0}^{2l-2}}{10^3\gamma_0\lambda\beta_{z0}^2}\left(\frac{l^l}{2^{l-1}l!}\right)^2\sigma_{\rm lin} = 1. \tag{7}$$

Where

$$\sigma_{\rm lin} = \left(\frac{\mu\theta}{4} - l\right)\exp\left(-\frac{\theta^2}{8}\right), \tag{8}$$

$$G_{\rm mn} = \frac{J_{\rm m-l}^2(u_{\rm mn}R_0/R_{\rm W})}{J_m^2(u_{\rm mn})(u_{\rm mn}^2 - m^2)}, \tag{9}$$

in which $\theta = (\omega - l\Omega_0)L/v_z$, ω is the resonant frequency, λ is the wavelength. Ω_0 is the relativistic cyclotron frequency, l is the number of operating harmonic of the cyclotron frequency, $\mu = \pi\beta_{\perp0}^2L/\beta_z\lambda$ is the parameter proportional to the effective length L of the cavity, $R_{\rm W}$ is the radius of the cavity, R_0 is the electron guiding centre radius, $\beta_{\perp0} = v_{\perp0}/c$ and $\beta_z = v_z/c$ are the normalized velocities of the transverse and longitudinal motion of the electrons, respectively, $I_{\rm st}$ is the starting current.

From Eq.(7) we can find that the dependence of the beam–wave coupling factor which indicates that the interaction between mode and electron beam on the beam radius has the following form:

$$\overline{I} \propto J_{\rm m-l}^2(u_{\rm mn}R_0/R_{\rm W}). \tag{10}$$

3. Cavity design

Figure 2 shows the coupling factor between electron beam and electromagnetic field in the cavities. From Fig.2, in the case of small R_0. the beam coupling to the mode with $m = l$ is much larger than that to all other modes. So, in order to improve the interaction between electron beam and electromagnetic field, we should choose the $\rm TE_{mn}$ mode satisfying $m = l$ as the operating mode in each cavity and the guiding centre radius R_0 being little greater than the larmor radius $R_{\rm L}$ of electron.

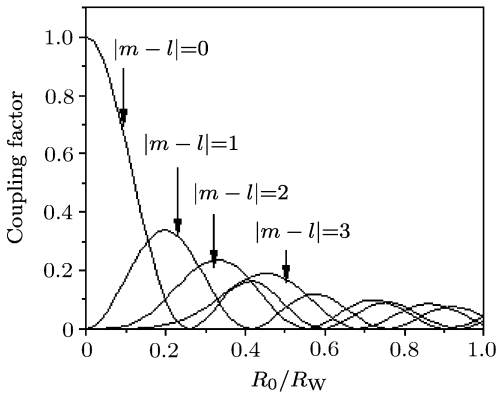


Fig.2. Coupling factor between beam and fields.

3.1. Input cavity

According to the above discussion, in the input cavity, the operating mode works at fundamental cyclotron harmonic, we can choose the $\rm TE_{11}$ mode as the operating mode. The resonant frequency of the $\rm TE_{11}$ mode calculated by the scattering matrices method is $f_0 = 55.36$ GHz. The distribution of the electric field simulated by CST software is shown in Fig.3.

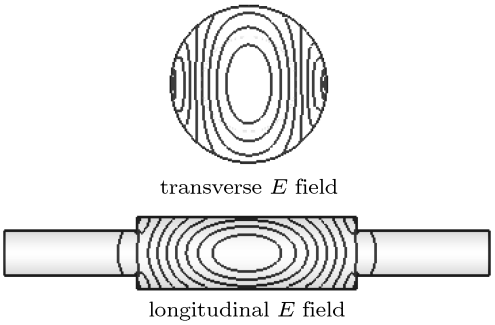


Fig.3. Distribution of the E field in the input cavity.

It was assumed that these devices are driven by an electron beam with a magnetic field $B_0 = 2.15$ T $V_0 = 40$ kV and an orbital-to-axial velocity ratio $\alpha = 1.5$. Figure 4 shows the dispersion diagram of the possible excited modes in the input cavity. From Fig.4, in the input cavity the possible parasitic mode is TE_{01} mode, which works at 2nd cyclotron harmonic. But the strong enough input electromagnetic field working at TE_{11} mode can suppress the possible parasitic mode effectively.

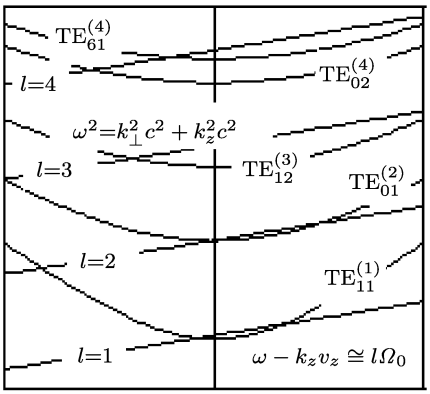


Fig.4. Dispersion diagram of the possible excited modes in the input cavity. (The superscript is the cyclotron harmonic number).

3.2. Bunching cavity

In the bunching cavity, the operating mode works at the 2nd cyclotron harmonic. TE_{21} mode can be chosen as the operating mode. The resonant frequency of TE_{21} mode is $f_0 = 111.9$ GHz. The electric fields distribution of TE_{21} simulated by CST software is shown in Fig.5.

From Fig.6, when the bunching cavity works at TE_{21} mode, the strong possible parasitic modes do not exist.

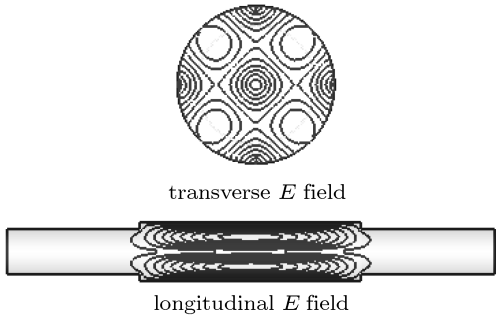


Fig.5. Distribution of E fields in the bunching cavity.

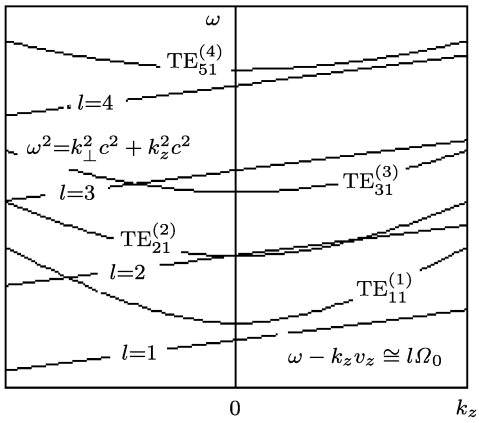


Fig.6. Dispersion diagram of the possible excited modes in the bunching cavity.

3.3. Output cavity

The operating mode works at the 4th cyclotron harmonic in the output cavity. So we should choose TE_{4n} mode as the operating mode. In order to get the optimal efficiency, we should design the output cavity to realize $Q_d/Q_o = 1/2$.[11] Using the scattering matrices method discussed above, we can obtain the resonant frequency, total quality factor and mode profile of the operating mode. Figure 7 shows the longitudinal field distribution of TE_{43} mode in the output cavity.

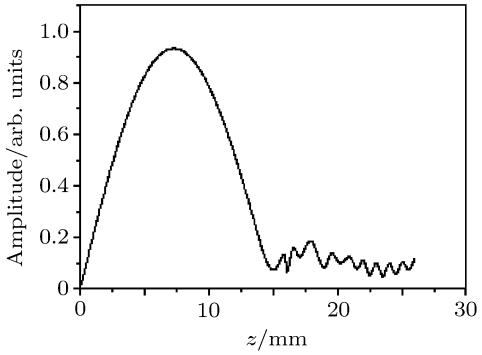


Fig.7. Longitudinal field distribution of TE_{43} mode in output cavity ($f_0 = 225$ GHz, $L_1 = 16$ mm, $L_2 = 10$ mm, $R_W = 2.69$ mm and $\phi = 8°$).

4. Starting current

The starting current is an important characteristic of any microwave source of coherent radiation. To realize efficient operation of an amplifier, it is advisable to operate at currents slightly below the starting current. Above it, the device will operate as a phase-locked oscillator in the presence of a driven signal. Meanwhile, it is also important to calculate the starting current of the possible parasitic modes for an amplifier because of the mode competition. Figure 8 shows the starting currents of the possible operating modes and the potential parasitic modes in output cavity.

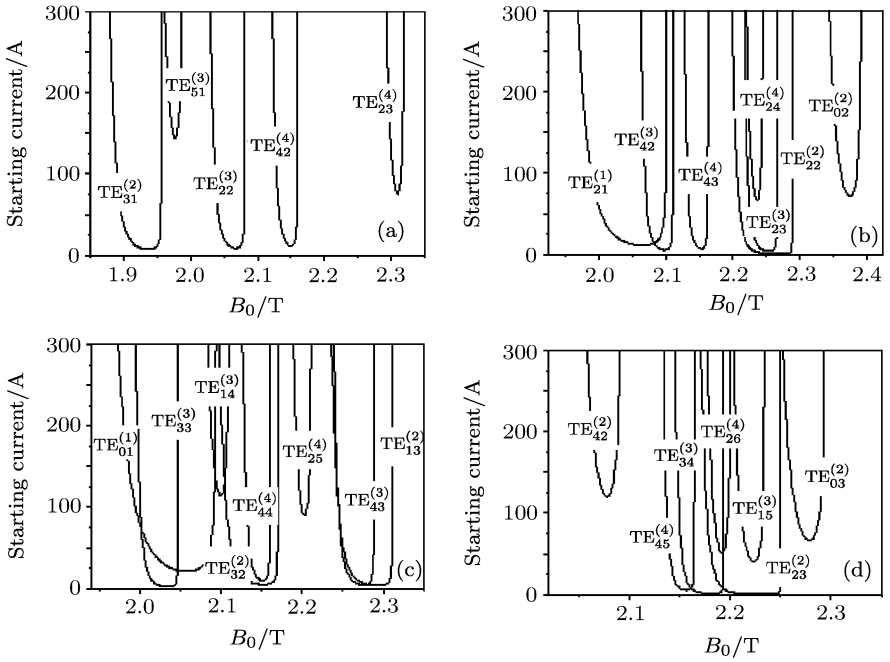


Fig.8. The starting current of the operating mode and possible parasitic mode in output cavity.(V_0 = 40 kV α = 1.5. (a) Operating mode: TE_{42} mode, (b) Operating mode: TE_{43} mode, (c) Operating mode: TE_{44} mode, (d) Operating mode: TE_{45} mode.

5. Discussion and conclusions

From Fig.8, when the output cavity of the frequency-quadrupling gyroklystron works at TE_{42} or TE_{43} mode, there are no strong possible parasitic modes at fundamental, second, third and fourth cyclotron harmonic, but when it works at TE_{44} mode, the TE_{32} mode working at 2nd harmonic is the possible competitive mode, when it works at TE_{45} mode, the possible competitive mode is TE_{34} mode working at 3rd harmonic. So, in order to eliminate the parasitic modes excitation in the output cavity, we should choose TE_{42} or TE_{43} mode as the operating mode. But under consideration of the power capacity, TE_{43} mode is the better choice.

In this article, we discuss the cavity design and operating mode selection of the frequency-quadrupling gyroklystron. In order to improve the interacting efficiency between electron beam and fields, we should choose the operating mode TE_{mn} satisfying $m = l$ in each cavity, meanwhile, the guide centre radius of the beam should be small enough to improve the efficiency and suppress the modes in the drift regions.

References

[1] Zhang K C, Wu Z H and Liu S G 2008 *Chin. Phys.* B **17** 3402

[2] Liu S G, Yuan X S, Fu W J, Yan Y, Zhang Y X, Li H F and Zhong R B 2007 *Phys. Plasmas* **14** 103113

[3] Liu S G, Yuan X S, Liu D W, Yan Y, Zhang Y X, Li H F and Zhong R B 2007 *Phys. Plasmas* **14** 103114

[4] Liu D W, Yuan X S and Liu S G 2008 *Fusion Engineering and Design* **83** 606

[5] Savilov A V and Nusinovich G S 2007 *Phys. Plasmas* **14** 053113

[6] Savilov A V and Nusinovich G S 2008 *Phys. Plasmas* **15** 013112

[7] Neilson J M, Latham P E, CapLan M and Lawson W G 1989 *IEEE Trans. Micro. Theory and Tech.* **37** 1165

[8] Liu S G 1987 *Realistic Electronics* (Beijing: Science press) p110

[9] Fliflet A W, Read M E, Chu K R and Seeley R 1982 *Int. J. Electronics* **53** 505

[10] Nusinovich G S and Li H F 1992 *Int. J. Electronics* **72** 895

[11] Zavolsky N A, Zapevalov V E and Moiseev M A 2006 *Radiophys. Quantum Electron.* **49** 108